

# Trionic optical potential for electrons in semiconductors

Martin J. A. Schuetz<sup>\*</sup>, Michael G. Moore and Carlo Piermarocchi

**Laser-induced optical potentials for atoms have led to remarkable advances in precision measurement, quantum information and towards addressing fundamental questions in condensed-matter physics. Here, we describe analogous optical potentials for electrons in quantum wells and wires that can be generated by optically driving the transition between a single electron and a three-body electron–exciton bound state, known as a trion. The existence of a bound trion state adds a term to the a.c. Stark shift of the material proportional to the light intensity at the position of the electron. According to our theoretical calculations, this shift can be large relative to the thermal equilibrium temperature of the electron, resulting in a relatively strong optical potential that could be used to trap, guide and manipulate individual electrons within a semiconductor quantum well or wire. These potentials can be thought of as artificial nanostructures on the scale of 100 nm that can be spin dependent and reconfigurable in real time. Our results suggest the possibility of integrating ultrafast optics and gate voltages in new resolved-carrier semiconductor optoelectronic devices, with potential applications in fields such as nanoelectronics, spintronics and quantum information processing.**

The optical properties of one- and two-dimensional semiconductor confined systems are dominated at low temperature by bound electron–hole pairs known as excitons<sup>1</sup>. In samples with a small excess of electrons, an exciton can capture another electron to form a charged exciton, or trion, which is the bound state of two electrons and a hole<sup>2,3</sup>. In good III–V and II–VI quantum-well samples, trions with high mobility have been observed<sup>4–6</sup>. From an atomic physics perspective, the electron to trion optical transition occurring in a semiconductor host environment effectively gives a second internal state to the electron, which is otherwise a point-like, structure-less particle in free space. Optically driving the transition between these two states then induces the electron to respond to the light in an atom-like manner.

When transitions between two internal atomic energy levels are driven by near-resonant laser light, the ground-state a.c. Stark shift is proportional to the laser intensity at the position of the atom. Thus, a spatially varying intensity pattern creates a spatially varying optical potential that acts on the atomic centre-of-mass motion. We propose creating analogous optical potentials for semiconductor charge carriers by driving the sample with light tuned near the trion resonance. A spatially inhomogeneous intensity profile will result in a mechanical potential acting on the electron (see Fig. 1). As a resonant effect, the trionic optical potential is many orders of magnitude stronger than the ponderomotive potential<sup>7</sup> that arises from the Lorentz force acting on the electron. In contrast to electron–hole pairs localized by transversal light forces<sup>8</sup>, an electron (or hole) in a trionic optical potential will not radiatively decay, opening the possibility for optical manipulation of charge flow and/or the creation of interesting many-electron states, for example, a solid-state quantum simulator<sup>9</sup>.

At present, we focus on the case of electrons confined in GaAs and CdTe quantum wells, as their optical properties have been most thoroughly investigated experimentally, but similar potentials should be obtainable for holes, as well as for carriers confined in quantum wires. A variational approach has been used to calculate the wavefunction and the optical properties of the three-particle

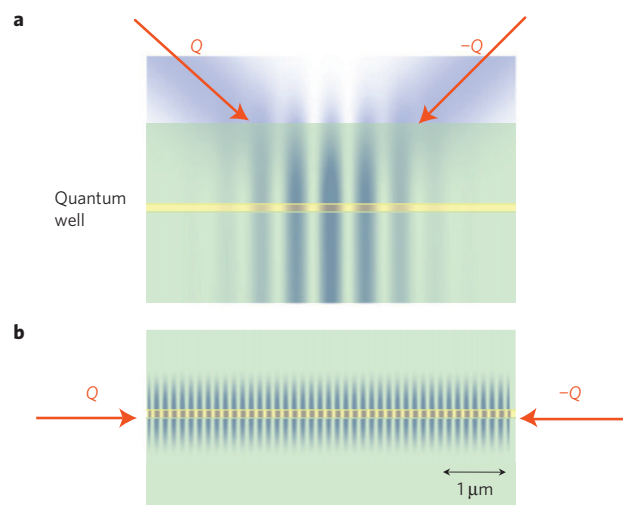


**Figure 1 | Interference pattern for two laser beams incident on the semiconductor structure. a**, Top excitation at incidence angle  $\pi/3$ . **b**, Lateral excitation. The interference pattern has been calculated using an average index of refraction  $n = 3.5$  corresponding to typical III–V-based structures. Note that the optical lattice periodicity can be partially controlled by changing the incidence angle.

trion state, as described in the Methods section. Under laser excitation, the electron makes virtual transitions into a bound trion state; while at the same time, the laser drives the transition to non-localized excitons. As these states are locally perturbed by the exciton–electron interaction, they can be viewed as ‘unbound trions’. Including both types of transition we have treated the light–matter coupling perturbatively and obtained a second-order effective Hamiltonian. We consider a monochromatic standing wave  $\mathbf{E}(\mathbf{r}, t) = \mathbf{E}_0 \cos(\mathbf{Q}\mathbf{r}) \cos(\omega t)$  containing photon modes with  $\pm Q$  in-plane momenta, producing an intensity pattern in the form of periodic stripes along the quantum well. Neglecting small

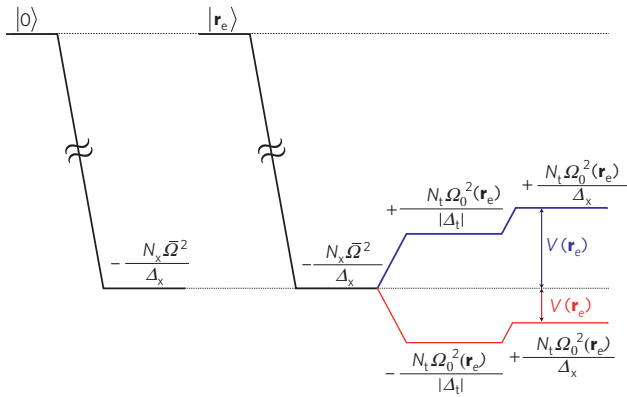


**Figure 2 | Scheme of energy-level shifts for an empty quantum well  $|0\rangle$  and for a quantum well with one electron at  $r_e$ , in the red- and blue-detuning case.** An exciton in a neutral quantum well, ideally coherent over the whole sample, has an oscillator strength that scales as  $N_x = A/A_x$ , where  $A$  is the total area of the sample and  $A_x$  is the exciton size. In contrast, the fact that a free carrier must be already present in the sample to create a trion implies that the trion oscillator strength scales as  $A_t/A_x = N_t$  (ref. 10), where  $A_t$  is an effective trion size. In the diagram the contributions from the bound trion (proportional to  $\Omega_0^2/\Delta_t$ ) and the continuum (proportional to  $\Omega_0^2/\Delta_x$ ) are shown separately.  $\Delta_{x(t)}$  is the photon-exciton (trion) detuning. Notice that the constant global energy shift  $-N_x \bar{\Omega}^2/\Delta_x$ , where  $\bar{\Omega}$  is a spatially averaged Rabi energy, does not contribute to the electron potential.

non-local effects (see the Methods section and Supplementary Fig. S1), the resulting potential for the electron can be expressed as

$$U(r) = -\varepsilon \Delta f_c(\Delta_t) \cos^2(\mathbf{Q} \cdot \mathbf{r})$$

where we introduce the dimensionless saturation parameter  $\varepsilon = \chi(\Omega_0/\Delta_t)^2$ . The parameter  $\Omega_0 = d_0|\mathbf{E}_0|$  is the Rabi energy, with  $d_0$  being the inter-band dipole moment, and  $\Delta_t$  is the difference between the trion resonance and the laser energy. The factor  $f_c(\Delta_t)$  is due to the presence of the continuum of unbound trions (see the Methods section), and can be approximated by  $f_c(\Delta_t) = E_b/(E_b + \Delta_t)$ , where  $E_b$  is the trion binding energy. As unbound excitons in our system would be equivalent to electron–positron excitations in the vacuum, we interpret this coefficient as a non-negligible vacuum polarizability correction. In the definition of the saturation parameter we include the coefficient  $\chi$  (see Supplementary Fig. S2), which is proportional to the integral over all configurations of the three-particle wavefunction with one electron and the hole taken at the same position<sup>10</sup>. The coefficient  $\chi$  is about 80 for GaAs and 90 for CdTe.

By decreasing the saturation  $\varepsilon$ , heating of the electron owing to spontaneous scattering of photons can be reduced. Photon scattering is enhanced by the trion resonance, occurring at the rate  $\Gamma_{se} = \varepsilon \Gamma_t$ , with  $\Gamma_t \sim 10^{10} \text{ s}^{-1}$  being the natural linewidth of the trion state. Whereas  $\Gamma_{se}$  scales as  $\sim 1/\Delta_t^2$ , the trap depth scales as  $f_c(\Delta_t)/\Delta_t$ . The sign of the trion–photon detuning  $\Delta_t$ , corresponds to two qualitatively different regimes for the optical potential (see Fig. 2). For red detuning,  $\Delta_t > 0$ , the potential minima are at the anti-nodes of the intensity profile, so that the electrons will be attracted towards high field intensities, where  $\Gamma_{se}$ , proportional the laser intensity, is maximum. The situation is reversed for intermediate blue detuning,  $\Delta_t < 0$ , where the potential minima correspond to the nodes of the standing-wave pattern, where  $\Gamma_{se}$  is minimized. We show in Fig. 3a,b the potential depth  $U_0$  for red and blue detuning as a function of the saturation parameter  $\varepsilon$ , which is proportional to the laser intensity. The detuning  $\Delta_t$  as well as the potential depth is represented in units of the trion binding

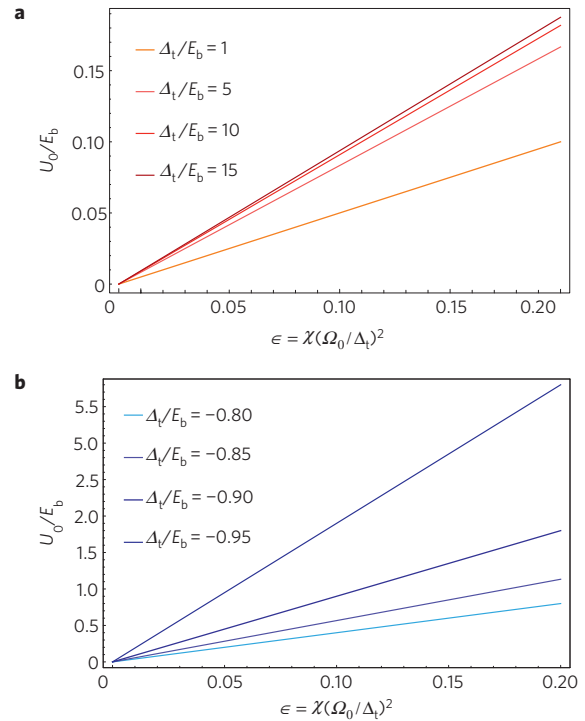


**Figure 3 | Potential depth as a function of laser intensity for various detunings. a, b,** Optical potential depths for red (a) and blue (b) detuning expressed in terms of the trion binding energy for different values of the optical detuning with respect to the trion resonance. In the red-detuned case the potential is attractive and electrons will be trapped at the anti-nodes of the interference pattern, whereas for blue detuning the potential is repulsive and electrons will be trapped at the nodes.

energy  $E_b$ , which is typically of the order of 2 meV in GaAs and 3.6 meV in CdTe semiconductor quantum wells. For red detuning, the continuum and the bound trion level give contributions of opposite sign to the shift of the electron ground-state energy (see Fig. 2). As a consequence, the potential depth saturates at a maximum of  $\varepsilon E_b$ . For intermediate blue detuning,  $E_b < |\Delta_t| < 0$ , the continuum and bound trion contributions add constructively, resulting in a significantly deeper potential, scaling as  $1/(E_b - |\Delta_t|)$ . The enhancement owing to the singularity at  $\Delta_t = -E_b$  is limited by the requirement to remain well outside the exciton resonance linewidth  $\Gamma_x$ , given for both GaAs and CdTe by approximately  $0.05E_b$ . For  $\varepsilon = 0.05$ , we find that a potential depth of  $0.5E_b$  is feasible. To realize this strong potential, laser intensities of  $I = 3 \times 10^3 \text{ W cm}^{-2}$  and  $I = 9 \times 10^3 \text{ W cm}^{-2}$  would be required for GaAs and CdTe quantum wells, respectively. These intensities are much weaker, for instance, than the ones used to observe the exciton Stark shift<sup>11</sup>, where a strong laser was followed by a weak probe to probe the energy difference between adjacent light-dressed states<sup>12</sup>. The optical potential, on the other hand, is simply the shift of the lowest dressed state, and is therefore much stronger.

A natural energy scale for quantifying the effects of laser heating is the single-photon recoil energy defined as  $E_R = \hbar^2 Q^2/2m_e^*$ , that is, the kinetic energy of an electron with a momentum equal to that of the laser photons and mass equal to the electron effective mass  $m_e^*$ . Translational invariance along the quantum well implies conservation of the in-plane momentum, which reduces the average recoil kick an electron experiences in the process of spontaneous photon emission. For GaAs and CdTe the in-plane kinetic energy imparted by photon recoil, averaged over the emission angle, is  $\langle E_R \rangle = 0.29 \text{ meV}$  and  $\langle E_R \rangle = 0.16 \text{ meV}$ , respectively. This is a conservative estimate neglecting the possibility of having part of

**Table 1 | Electron equilibrium temperature in K for GaAs and CdTe for different values of the saturation parameter.**

	GaAs (K)	CdTe (K)
$\varepsilon = 0.10$	4.6	2.9
$\varepsilon = 0.05$	3.5	2.3
$\varepsilon = 0.01$	2.3	1.2

Equilibrium temperature resulting from the balance of laser heating and phonon cooling for different saturation parameters for the two materials. The lattice temperature is 300 mK (see also Supplementary Fig. S4).

the recoil momentum transferred to phonons. The small effective mass of the electron—which is about seven orders of magnitude smaller than the mass of rubidium atoms—gives rise to relatively large recoil energies. However, this energy has to be compared with the maximum achievable depth of the trionic optical potential, which is significantly deeper than atomic potentials owing to a much higher oscillator strength, as well as the enhancement owing to the background polarizability. We compare our potential-depth to recoil-energy ratio with three typical atomic optical lattice experiments on macroscopic quantum interference<sup>13</sup>, Bloch oscillations<sup>14</sup> and quantum phase transitions<sup>15</sup>. The maximum achievable potential depths in these experiments have been  $2.1E_R$ ,  $6E_R$  and  $22E_R$ , respectively. Despite the large recoil energies involved in our system, we predict potential depths of about  $3E_R$  and  $10E_R$  for GaAs and CdTe, respectively. For CdTe, we have also estimated the number of quasi-bound states by approximating the trapping potential as a single harmonic oscillator and comparing the energy-level separation to the total depth. We found that three levels are bound within a large range of detuning and saturation parameters.

In contrast to the case with trapped atoms, cooling of the electron is provided by a mechanism completely separate from the optical trapping mechanism: coupling to the phonon reservoir. In our energy range, the electrons will cool down by acoustic phonon emission (Supplementary Fig. S3). The equilibrium temperature is therefore determined by competition between phonon emission and laser heating (we assume that the experiment will be carried out at 300 mK, where phonon absorption can be neglected). The laser heating rate  $R_h$ —measured in energy per time—can be expressed as  $R_h = \varepsilon \Gamma_t(E_R)$ , whereas acoustic phonon emission tends to cool the electron down at some cooling rate  $R_c(E)$ . The two competing processes lead to an effective equilibrium energy defined by  $R_c(E_{eq}) = R_h$  (Supplementary Fig. S4). Using the electron–phonon deformation potential interaction, a lattice temperature of 300 mK and a quantum-well width of 20 nm we have calculated cooling and heating rates and the effective equilibrium electron temperature for different values of the saturation  $\varepsilon$  (Table 1). For  $\varepsilon = 0.05$  and  $\Delta_t = -0.9E_b$ , we predict a potential depth of  $0.5E_b$ , corresponding to 1 meV for GaAs and 1.8 meV for CdTe. The depth of the trapping potential thus exceeds the electron equilibrium temperature by up to one order of magnitude.

In the blue-detuned case, the possibility arises for phonon-assisted photon absorption. Virtual trions created by photon absorption can decay into real trions by acoustic phonon emission. This occurs at a rate of the order of  $0.8 \text{ ns}^{-1}$  in homogeneously illuminated GaAs samples with  $\varepsilon = 0.05$  (Supplementary Fig. S3). We note that, in the blue-detuned case electrons are confined in the vicinity of the nodes of the intensity pattern, which will further suppress both the photon and phonon emission rates by a factor that can be analytically calculated as  $(1 - e^{-\sqrt{E_b/U_0}})/2$ . Note that although the resulting real trion will decay by spontaneous photon emission, and thus lead to an increase in the heating rate, the emitted photons will be at the trion resonance frequency. This raises the possibility of measuring the electron density by imaging the light

at the trion resonance frequency, as this light will be emitted only in proximity to an electron.

As a result of spin–orbit interaction and confinement, the trion level structure allows spin-up electrons to respond only to right-handed photons, whereas spin-down electrons see only left-handed photons (see Supplementary Fig. S5). This means that the trionic optical potentials for spin-up and spin-down electrons, generated by left- and right-circularly polarized laser fields, respectively, can be completely independent of each other. Thus, it might be possible to generate entanglement between an electron's spin and orbital motions. This could then be used to generate entanglement between the spins of two neighbouring electrons, as their separation, and therefore interaction strength, can depend strongly on the spin states of the individual electrons. These possibilities show that, when viewed either as a platform for addressing fundamental open questions in condensed-matter physics, and/or as a platform for spin-based quantum information processing, optically trapped charged particles in a semiconductor environment are not intrinsically disadvantageous with respect to their atomic cousins.

In future work, we will consider optical potentials for heavy holes, which have a reduced heating rate owing to their larger mass; as well as for bi-layer excitons<sup>16</sup>, which have the advantage of being electrically neutral, and thus interact at a much shorter range than either electrons or holes. We will also explore the possibility for even deeper potentials in quantum wires, where confinement in two dimensions should lead to even stronger enhancement.

## Methods

**Charge loading.** The loading of charges in the optical potential could be experimentally realized using different techniques. The electronic density has to remain low to limit Coulomb effects, ideally around  $10^9 \text{ cm}^{-2}$ , corresponding to a Fermi energy of about 0.02 meV, much smaller than the optical potential depth. The quantum well could be embedded in a Schottky diode structure controlled by an external d.c. field. This method has been used in loading layers of quantum dots with one electron each<sup>17</sup>. Realizations relying on delta doping layers may present problems owing to ionized doping centres, which generate a random potential in the plane of the quantum well. However, according to direct scanning probe techniques, this potential is characterized by patterns with dominant length scales of the order of one micrometre<sup>18</sup> and we expect that electron trapping could be created inside these micrometre-sized patterns. As we need a low carrier density, the sample design can be optimized to minimize the effect of ionized impurities. For instance, the dopant layers could be made thick and relatively distant from the optical potential region. Charge loading could also be realized by photo-doping double-quantum-well systems. Here, spatially separated electrons and holes are created following high-energy excitation. For distant quantum wells the charges can remain confined for seconds<sup>19</sup> and we could obtain two independent optical potentials for the two types of carrier. For smaller separation of the wells the optical potential will trap indirect excitons and could complement other methods of controlling indirect exciton fluxes in integrated circuits<sup>16</sup>. Finally, one could simply take advantage of unintentional doping in the barriers, and pump with an energy just above the ionized acceptor to conduction transition in the barriers to produce electrons that relax in a single quantum well, as recently demonstrated<sup>20</sup>.

**Competing effects.** We have studied the possibility of optical excitation of the electron out of the confining quantum well. This process competes with virtual trion formation, but the corresponding matrix element is vanishingly small owing to the mismatch between the two-dimensional wavefunction in the quantum well and the extended bulk-like states in the barriers. An upper bound estimation of the branching ratio between electron ionization and trion creation in the quantum well, neglecting Coulomb enhancement effects, gives  $10^{-5}$ . We have also considered disorder effects owing to fluctuations in the number of atomic monolayers. These fluctuations create islands corresponding to different well or wire widths. The optical potential will not be affected if the characteristic length of the islands is much smaller or much larger than the carrier confinement length. From this point of view, a promising system for the experimental realization is represented by V-groove semiconductor quantum wires, in which one-dimensional islands of the order of  $1 \mu\text{m}$  and extremely narrow homogeneous emission lines have been explicitly observed<sup>21,22</sup>. In wires, the trion binding energy and thus the optical potential will be larger than the one calculated above. In principle very high-quality quantum wells without growth interruption should feature large islands similar to the ones in quantum wires. For relatively large quantum wells with a width of around 20 nm, the exciton linewidths can be extremely narrow. For instance, 25 nm

quantum wells with exciton lines of 0.075 meV have been reported<sup>23</sup>. In those samples the effect of interface disorder is completely negligible. Alloy disorder is also present, but owing to its extremely short-range characteristic length<sup>24</sup> its effects are averaged out within the electron envelope function. Finally, unintended doping can contribute to the absorption through impurity-bound exciton resonances and their phonon satellites lines. However, absorption of energy owing to unintended doping mostly occurs in the barriers and substrate, and is significant only at energies quite higher than the quantum-well trion resonance.

**Detection schemes.** The detection of electrons trapped by the optical potential can be realized by detecting the weak optical emission at the trion energy, which will be spectrally separated from emission at the pump energy. The emission at the trion energy at a given spot is a signature of the presence of the electron. In the blue-detuning case the trion emission will occur at the dark spots of the pump interference pattern and should be less challenging to observe. Both far-field and near-field optical techniques should be able to demonstrate the carrier localization. In contrast to atomic systems, the confined carriers are charged, and charge-imaging methods could also be used to detect electrons trapped by the optical potential in a way similar to the detection of single electrons trapped by impurity centres<sup>25</sup>. We note that the experiments we propose are very similar to four-wave-mixing experiments that have been carried out in two-dimensional electron gas systems (for a review see ref. 26). The only difference is that we are proposing to explore a different regime of carrier density and excitation energy.

**Variational calculation.** For the trion state ( $X^-$ ) we have used a two-dimensional variational Hylleraas function<sup>27</sup> of the form  $\varphi_b(s, t, u) = N e^{-\alpha s} (1 + \beta u + \gamma t^2)$ , where  $\alpha$ ,  $\beta$  and  $\gamma$  are three variational parameters and  $N$  is the normalization constant. The position of the three carriers in the trion is expressed in terms of two elliptic coordinates  $s = r_{e_1h} + r_{e_2h}$  and  $t = r_{e_1h} - r_{e_2h}$  and the inter-electron distance  $u = r_{e_1e_2}$ . Hylleraas-type wavefunctions are known to accurately describe radial and internal angular correlation effects<sup>28</sup>. For GaAs and CdTe quantum wells we have obtained trion binding energies of about 2.05 meV and 3.6 meV, respectively, which is in good agreement with the experiments<sup>6</sup>. Using this wavefunction we have found radiative lifetimes of about 20 ps for both materials, also in reasonable agreement with the experimental values<sup>5</sup>.

The matrix element for the optical transition from an initial electron with momentum  $\mathbf{k}$  to a bound trion state with centre-of-mass momentum  $\mathbf{K}$  can be written as

$$\langle \mathbf{K} | H_{LM} | \mathbf{k} \rangle = \frac{\Omega_0}{2} [\delta_{\mathbf{K}, \mathbf{k} + \mathbf{Q}} I(\beta_X \mathbf{k} - \beta_e \mathbf{Q}) + \delta_{\mathbf{K}, \mathbf{k} - \mathbf{Q}} I(\beta_X \mathbf{k} + \beta_e \mathbf{Q})] \quad (1)$$

where the first and second terms on the right-hand side describe the absorption of a photon in the  $+\mathbf{Q}$  mode and in the  $-\mathbf{Q}$  mode, respectively. The coefficient  $\beta_e = 1 - \beta_X = m_e/m_t$  is the electron to trion mass ratio, the light-matter interaction is indicated by  $H_{LM}$  and  $\Omega_0$  is the Rabi energy. The quantity  $I(\mathbf{p}) = (1/\sqrt{2\pi}) \int d\mathbf{r} e^{-i\mathbf{p}\cdot\mathbf{r}} \varphi_b(r, r, r)$  is the Fourier transform of the bound trion wavefunction  $\varphi_b$  taken with one electron and the hole at the same position. This function enters in equation (1) with  $\mathbf{p} = \beta_X \mathbf{k} \pm \beta_e \mathbf{Q}$ , which is the relative momentum of the initial electron  $\mathbf{k}$  and the photo-created exciton with  $\pm\mathbf{Q}$ . For the calculation of the optical potentials we have used a full analytical expression for the function  $I(\mathbf{p})$  (ref. 29). Note that the enhancement factor is approximately given by  $\chi = |I(\mathbf{p} = 0)|^2$ .

**Perturbation theory.** The second-order effective Hamiltonian for the electron can be written as

$$H_{\text{eff}} = P_e \sum_{\mathbf{k}} (\varepsilon_{\mathbf{k}}^{(0)} + \varepsilon_{\mathbf{k}}^{(2)}) |\mathbf{k}^{(0)}\rangle \langle \mathbf{k}^{(0)}| + \varepsilon_{\mathbf{k}}^{(0)} (|\mathbf{k}^{(0)}\rangle \langle \mathbf{k}^{(2)}| + |\mathbf{k}^{(2)}\rangle \langle \mathbf{k}^{(0)}|) P_e \quad (2)$$

where the subscripts (0) and (2) indicate the zeroth- and second-order corrections to the electron energy  $\varepsilon_{\mathbf{k}}$  and wavefunction  $|\mathbf{k}\rangle$  with respect to the light-matter coupling, and  $P_e$  is a projector on single-electron states. The second term on the right-hand side of equation (2) includes off-diagonal processes between electronic states with different  $\mathbf{k}$  owing to the mixing with photon modes. These off-diagonal contributions can be written in the form

$$H_{\text{OD}} = \left[ -\sum_{\mathbf{k}} \frac{\Omega_0^2}{4} \left( \frac{1}{\Delta_t} + \frac{\chi_e(\Delta_x)}{\Delta_x} \right) |I(\mathbf{k})|^2 + \frac{\Omega_0 \Omega_X}{\Delta_x} O(\mathbf{K}, \mathbf{k}) I(\mathbf{k}) \right] \times |\mathbf{k} - \mathbf{Q}\rangle \langle \mathbf{k} + \mathbf{Q}| + h.c.$$

where  $\Delta_{x(t)}$  is the photon-exciton (trion) detuning,  $O(\mathbf{K}, \mathbf{k}) = \langle \mathbf{K} | \mathbf{K}, \mathbf{k} \rangle$  is the overlap between a bound state trion with centre-of-mass momentum  $\mathbf{K}$  and an unbound state composed of one exciton with centre-of-mass momentum  $\mathbf{K}$  and one electron of momentum  $\mathbf{k}$  and  $\Omega_X$  is the Rabi energy modified by excitonic effects. We have defined the quantity  $\chi_e(\Delta)/\Delta = \sum_{\mathbf{k}} \langle O(0, \mathbf{k}^2) \rangle / \hbar^2 k^2 / 2\mu_t + \Delta$ , where  $\mu_t$  is the reduced mass of the free-exciton/free-electron system. These

off-diagonal terms are the dominant terms in the derivation of a potential that carries the signature of the intensity profile. From the effective Hamiltonian in  $\mathbf{k}$ -space, we derive a Schrödinger equation for the electron wavefunction  $\psi(\mathbf{r})$  in the presence of the standing wave given by

$$-\frac{\hbar^2 \nabla^2}{2m_e^*} \psi(\mathbf{r}) - \frac{\Omega_0^2}{\Delta_t} f_c(\Delta_t) \int d\mathbf{r}' \cos^2 \left( \mathbf{Q} \frac{\mathbf{r} + \mathbf{r}'}{2} \right) m(\mathbf{r} - \mathbf{r}') \psi(\mathbf{r}') = E \psi(\mathbf{r})$$

We note that the optical potential is not diagonal in coordinate representation; rather it depends on the non-local kernel  $m(\mathbf{r} - \mathbf{r}')$ . The continuum factor and non-local kernel are new effects related to the vacuum polarizability of the electron's environment, and are not observed in atomic systems. A plot of the kernel function  $m(\mathbf{x})$  is shown in Supplementary Fig. S1, where we see that it matches the size of the trion bound state. As the size of the kernel is small compared with the optical wavelength, non-local effects can be treated as a perturbation that effectively averages the light intensity over a small area centred on the electron position, corresponding to the approximation  $m(\mathbf{x}) = \chi \delta(\mathbf{x})$ . In practical terms, the non-locality will limit the obtainable electron localization to the trion length scale, even if significantly deeper potentials than we consider might somehow be realized.

Received 8 July 2010; accepted 9 August 2010; published online 26 September 2010

## References

- Burstein, E., Weisbuch, C. & North Atlantic Treaty Organization Scientific Affairs Division, *Confined Electrons and Photons: New Physics and Applications* (Plenum Press, 1995).
- Lampert, M. A. Mobile and immobile effective-mass-particle complexes in nonmetallic solids. *Phys. Rev. Lett.* **1**, 450–453 (1958).
- Finkelstein, G. *et al.* Charged exciton dynamics in GaAs quantum wells. *Phys. Rev. B* **58**, 12637–12640 (1998).
- Sanvitto, D. *et al.* Observation of charge transport by negatively charged excitons. *Science* **294**, 837–839 (2001).
- Ciulin, V. *et al.* Radiative lifetime of negative trions in GaAs and CdTe quantum wells. *Phys. Status Solidi A* **178**, 495–499 (2000).
- Bar-Joseph, I. Trions in GaAs quantum wells. *Semicond. Sci. Technol.* **20**, R29–R39 (2005).
- Freeman, R. R., Bucksbaum, P. H. & McIlrath, T. J. The ponderomotive potential of high-intensity light and its role on the multiphoton ionization of atoms. *IEEE J. Quantum Electron.* **24**, 1461–1469 (1988).
- Binder, R. & Lindberg, M. Optical electron-hole tweezers in semiconductors. *J. Phys. Condens. Matter* **18**, 729–740 (2006).
- Feynman, R. P. Simulating physics with computers. *Int. J. Theor. Phys.* **21**, 467–488 (1982).
- Combescot, M. & Tribollet, J. Trion oscillator strength. *Solid State Commun.* **128**, 273–277 (2003).
- Mysyrowicz, A., Hulin, D., Antonetti, A. & Migus, A. Dressed excitons in a multiple-quantum-well structure—evidence for an optical stark-effect with femtosecond response-time. *Phys. Rev. Lett.* **56**, 2748–2751 (1986).
- Combescot, M. & Combescot, R. Excitonic stark shift—a coupling to semivirtual biexcitons. *Phys. Rev. Lett.* **61**, 117–120 (1988).
- Anderson, B. P. & Kasevich, M. A. Macroscopic quantum interference from atomic tunnel arrays. *Science* **282**, 1686–1689 (1998).
- BenDahan, M., Peik, E., Reichel, J., Castin, Y. & Salomon, C. Bloch oscillations of atoms in an optical potential. *Phys. Rev. Lett.* **76**, 4508–4511 (1996).
- Greiner, M., Mandel, O., Esslinger, T., Hansch, T. W. & Bloch, I. Quantum phase transition from a superfluid to a Mott insulator in a gas of ultracold atoms. *Nature* **415**, 39–44 (2002).
- High, A. A., Novitskaya, E. E., Butov, L. V., Hanson, M. & Gossard, A. C. Control of exciton fluxes in an excitonic integrated circuit. *Science* **321**, 229–231 (2008).
- Ware, M. E. *et al.* Polarized fine structure in the photoluminescence excitation spectrum of a negatively charged quantum dot. *Phys. Rev. Lett.* **95**, 177403 (2005).
- Chakraborty, S., Maasilta, I. J., Tessmer, S. H. & Melloch, M. R. Imaging a two-dimensional electron system with a scanning charged probe. *Phys. Rev. B* **69**, 073308 (2004).
- Lundstrom, T., Schoenfeld, W., Lee, H. & Petroff, P. M. Exciton storage in semiconductor self-assembled quantum dots. *Science* **286**, 2312–2314 (1999).
- Portella-Oberli, M. T. *et al.* Dynamics of trion formation in  $\text{In}_x\text{Ga}_{1-x}$ As quantum wells. *Phys. Rev. Lett.* **102**, 096402 (2009).
- Guillet, T., Grousson, R., Voliotis, V., Wang, X. L. & Ogura, M. Local disorder and optical properties in V-shaped quantum wires: Toward one-dimensional exciton systems. *Phys. Rev. B* **68**, 045319 (2003).
- Crotini, A., Staehli, J. L., Deveaud, B., Wang, X.-L. & Ogura, M. Near-field imaging of one-dimensional excitons delocalized over mesoscopic distances. *Phys. Rev. B* **63**, 121313 (2001).

23. Langbein, W. & Hvam, J. M. Dephasing in the quasi-two-dimensional exciton-biexciton system. *Phys. Rev. B* **61**, 1692–1695 (2000).
24. Ropers, C. *et al.* Atomic scale structure and optical emission of  $\text{Al}_x\text{Ga}_{1-x}\text{As}/\text{GaAs}$  quantum wells. *Phys. Rev. B* **75**, 115317 (2007).
25. Kuljanishvili, I. *et al.* Scanning-probe spectroscopy of semiconductor donor molecules. *Nature Phys.* **4**, 227–233 (2008).
26. Broocks, K. A. *et al.* Linear and ultrafast optical spectroscopy in the regime of the quantum Hall effect. *Phys. Status Solidi B* **245**, 321–330 (2008).
27. Bethe, H. A. & Salpeter, E. E. *Quantum Mechanics of One- and Two-Electron Atoms* (Springer-Verlag: Academic, 1957).
28. Flores-Riveros, A. Generalized Hylleraas-Gaussian basis sets applied to the variational treatment of two-electron atoms. *Int. J. Quantum Chem.* **66**, 287–300 (1998).
29. Schuetz, M. J. A. *Trionic Optical Potentials for Charge Carriers in Semiconductors* (Michigan State University, 2009).

## Acknowledgements

We thank C. W. Lai and S. H. Tessmer for discussions on the experimental realizations. We acknowledge support by the National Science Foundation (C.P., M.G.M. and M.J.A.S.), the German Studienstiftung Program (M.S.) and the Fulbright Foundation (M.J.A.S.).

## Author contributions

M.J.A.S. carried out calculations; C.P. and M.G.M. proposed the concept; C.P., M.G.M. and M.J.A.S. wrote the manuscript.

## Additional information

The authors declare no competing financial interests. Supplementary information accompanies this paper on [www.nature.com/naturephysics](http://www.nature.com/naturephysics). Reprints and permissions information is available online at <http://npg.nature.com/reprintsandpermissions>. Correspondence and requests for materials should be addressed to M.J.A.S.